

result of a fluctuation of composition in the first coordination sphere. Fluctuations of concentration produce spin-density fluctuations, which develop into long-range antiferromagnetic order with increase of the Fe content. The basic nuclei of the antiferromagnetic state are clusters composed solely of Fe atoms. These results agree well with Sedov's paper,²² where it was shown that the magnetic state of the Fe atom in the γ phase is determined by its nearest environment and that for certain neighborhoods the value of μ_{Fe} tends to zero.

Atoms of Mn promote the development of the antiferromagnetic state and accelerate the ferro-antiferromagnetic transition. But only a part of the Cr and V atoms participate in the formation of clusters with short-range antiferromagnetic order, and this leads, at insufficient concentrations of Fe, to a concentration-al ferro-paramagnetic transition.

The martensitic transformation that occurs in the Fe-Ni system affects the antiferromagnetic state in the residual γ phase and slows down the ferro-antiferromagnetic transition. Since the production of an antiferromagnetic state begins in the Invar range of compositions, it causes so-called Invar anomalies of the properties, one of which (a decrease of $\bar{\mu}$) is described by the proposed cluster model.

The authors thank I. M. Ivanova for carrying out the micro-x-ray spectral analysis of the specimens, and G. B. Kurdyumov, I. M. Puzei, I. L. Aptekar', I. Ya. Georgieva, and Ya. M. Golovchiner for useful discussions of the results of the research.

¹M. Shiga, J. Phys. Soc. Jap. **22**, 539 (1967).

²S. Kachi and H. Asano, J. Phys. Soc. Jap. **27**, 536 (1969).

³V. I. Goman'kov, E. V. Kozis, and B. N. Mokhov, Dokl. Akad. Nauk SSSR **225**, 807 (1975) [Sov. Phys. Dokl. **20**, 843 (1975)].

⁴B. N. Mokhov, V. I. Goman'kov, and I. M. Puzei, Pis'ma Zh. Eksp. Teor. Fiz. **25**, 299 (1977) [JETP Lett. **25**, 274 (1977)].

⁵V. I. Goman'kov, B. N. Mokhov, and E. I. Mal'tsev, Pis'ma Zh. Eksp. Teor. Fiz. **23**, 97 (1976) [JETP Lett. **23**, 83 (1976)].

⁶Amorphous Magnetism II (ed., R. A. Levy and R. Hasegawa), Plenum Press, N. Y., 1977.

⁷A. Z. Men'shikov, V. A. Kazantsev, and N. N. Kuzmin, Zh. Eksp. Teor. Fiz. **71**, 648 (1976) [Sov. Phys. JETP **44**, 341 (1976)].

⁸A. Z. Men'shikov, S. K. Sidorov, and A. E. Teplykh, Fiz. Met. Metalloved. **45**, 949 (1978).

⁹V. Jacrot and T. Riste, in: Scattering of Thermal Neutrons, ed. P. A. Egelstaff, Academic, 1965 [Russ. Transl., Atomizdat, 1970, p. 253].

¹⁰Y. Nakamura and N. Miyata, J. Phys. Soc. Jap. **23**, 223 (1967).

¹¹Y. Nakamura, Y. Takeda, and M. Shiga, J. Phys. Soc. Jap. **25**, 287 (1968).

¹²I. M. Puzei and V. V. Sadchikov, Fiz. Met. Metalloved. **41**, 1099 (1976) [Phys. Met. Metallogr. **41**, No. 5, 181 (1976)].

¹³L. Kaufman and M. Cohen, Thermodynamics and Kinetics of Martensitic Transformations. In: Progress in Metal Physics (ed. B. Chalmers and R. King), Vol. 7, Pergamon Press, 1958, pp. 165-246 (Russian tr., Metallurgizdat, 1961).

¹⁴R. G. Davies and C. L. Magee, Met. Trans. **1**, 2927 (1970).

¹⁵G. F. Bolling, A. Arrott, and R. H. Richman, Phys. Status Solidi **26**, 743 (1968).

¹⁶J. Crangle and G. C. Hallam, Proc. R. Soc. A **272**, 119 (1963).

¹⁷S. Chikazumi, T. Mizoguchi, N. Yamaguchi, and P. Beckwith, J. Appl. Phys. **39**, 939 (1968).

¹⁸Y. Ishikawa, Y. Endoh, and T. Takimoto, J. Phys. Chem. Solids **31**, 1225 (1970).

¹⁹Y. Nakamura, M. Shiga, and Y. Takeda, J. Phys. Soc. Jap. **27**, 1470 (1969).

²⁰Y. Endoh and Y. Ishikawa, J. Phys. Soc. Jap. **30**, 1614 (1971).

²¹S. C. Abrahams, L. Guttman and J. S. Kasper, Phys. Rev. **127**, 2052 (1962).

²²V. L. Sedov, Zh. Eksp. Teor. Fiz. **74**, 2066 (1978) [Sov. Phys. JETP **47**, 1074 (1978)].

Translated by W. F. Brown, Jr.

Dilatometric investigation of critical phenomena in the ferroelectric phase transition in antimony sulfoiodide SbSI

A. N. Zisman,¹⁾ V. N. Kachinskii, V. A. Lyakhovitskaya, and S. M. Stishov

Crystallography Institute, USSR Academy of Sciences

(Submitted 19 December 1978)

Zh. Eksp. Teor. Fiz. **77**, 640-651 (August 1979)

A capacitive dilatometer is used to investigate in detail the ferroelectric phase transition in single crystal antimony sulfoiodide SbSI at pressure up to 5 kbar. The coordinates of the polycritical point were found to be $T = 233 \pm 5$ K and $P = 1430 \pm 100$ bar. An analysis of the experimental data yielded within the limits of the experimental accuracy a value 0.5 for the exponent α , in agreement with the Landau theory for the case of the tricritical point.

PACS numbers: 77.80.Bh, 64.60.Kw

At first shown by Landau,¹ the line of first-order phase transitions can terminate at a critical point of a singular type, wherein the phase does not vanish at all, as in the case of the critical point on the evaporation curve, but becomes a second-order phase transition. The possibility of the existence of crit-

ical points of this type follows from the Landau expansion

$$\Phi = \Phi_0 + A\eta^2 + B\eta^4 + D\eta^6 + \dots, \quad (1)$$

a second-order phase transition occurs at $B > 0$, a first order transition at $B < 0$, and the critical point

corresponds to $B=0$. The physical causes of the vanishing of the coefficient B are connected with interaction of the order parameter with other extensive variables that determine the state of the crystal.²

The first to point out the possible existence of a critical point on a phase transition curve were Volk, Gerzanich, and Fridkin³ who investigated the shift of the absorption edge in SbSI at high pressure. Direct proof of the existence of a critical point on a phase-transition curve was obtained by Garland and Weiner⁴ in a dilatometric investigation of a phase transition in NH_4Cl at high pressure. Griffiths⁵ has shown later that a large number of seemingly unrelated phenomena, such as the critical stratification point in the He^3 - He^4 mixture and critical phenomena in certain magnetic systems can be described in fact in equivalent terms, and introduced the concept of the tricritical point, which corresponds precisely to the case considered by Landau.¹ Introduction of this term might seem unnecessary were it not for the possibility of vanishing of terms of order higher than the fourth in (1), and of the onset of critical points of higher order. Such a possibility was discussed, in particular, for the critical point of NH_4Cl .⁶ Definite proof was obtained recently of the existence of polycritical points for phase transitions in KDP (Ref. 7) and in barium titanate.⁸

A characteristic feature of critical points of this type, or polycritical points, is that even within the framework of the Landau expansion (1) the second derivatives of the thermodynamic potential, which describe the behavior of the heat capacity, of the compressibility, and of the thermal-expansion coefficient, have a singularity at the transition point and can be represented in an ordered phase in the form

$$\chi = \chi_0 + \chi_1 \left| \frac{T - T_c}{T_c} \right|^{-\alpha}, \quad (2)$$

where T_c is the temperature of the polycritical point and χ_0 is the regular part of the corresponding quantity.

The value of the exponent α is determined by the order of the first nonzero term of the expansion; in particular, $\alpha = 0.5$ at the tricritical point. It is of interest that at the tricritical point ($B=0$) the fluctuations turn out to be suppressed to a considerable degree,⁹ so that it is possible to investigate the polycritical phenomena within Landau's classical approach even in a region quite close to the transition point. This is all the more true in the case of uniaxial ferroelectrics, such as the SbSI investigated in the present paper, in which the fluctuation region is in any case narrow.¹⁰

The results of the earlier investigations of the critical phenomena in SbSI at high pressures are quite contradictory. Soon after the publication of the cited paper by Volk, Gerzanich, and Fridkin,³ Syrkin *et al.*¹¹ performed dielectric measurements of polycrystalline SbSI samples in the region of the ferroelectric phase transition at high pressure and found no corroboration of the results of Ref. 3, that a critical point exists on the phase-transition point in this substance. Later on

Samara¹² performed dielectric measurements of SbSI single crystals and found likewise no convincing proof favoring the existence of a critical point. Subsequently, however, Peercy,¹³ in an investigation of light scattering in SbSI at high pressures, concluded that a critical point does exist on the curve of the phase transition in SbSI. Most recently Samara¹⁴ also came around to this point of view after repeating the measurements of the dielectric constant in crystals of better quality.

It seemed important therefore to carry out a thermodynamic investigation of the phase transition in SbSI for the purpose of reliably establishing the existence of a polycritical point and of studying the behavior of the thermodynamic quantities in the critical region.

EXPERIMENTAL PROCEDURE

We measured in these experiments the thermal expansion and compressibility of SbSI single crystals along the c axis using a capacitive dilatometer. The dilatometer together with the sample were placed in a high-pressure vessel placed in turn in a nitrogen cryostat.

Three single-crystal samples obtained by two different methods were investigated. Samples 1 and 2 were grown from the gas phase in a horizontal resistance furnace from previously synthesized polycrystalline material to which water was added as the transporter. These samples had natural faceting—the prism face (110) and the pinacoid faces (010) and (100). The end faces of the crystal were cut along the (001) plane. Sample 3 was part of a splice of several single-crystal blocks obtain from the melt by the Bridgman-Stockbarger method in an evacuated glass ampoule. A disk was sawn from the ingot, and the single crystal was chipped from the disk along the (110) cleavage plane. The crystals were sawed with a filamentary saw using an alkali solvent. All the samples were rectangular prisms with generators parallel to the [001] axis, 3–6 mm high, and $\sim 2 \times 2$ mm base.

The samples were placed in a dilatometer with a capacitive displacement sensor; the schematic diagram of the dilatometer is shown in Fig. 1. The sensor operates in the following manner. The change of length of sample 1 causes movable electrode 2 to move and to form with immobile electrode 3 a capacitor C_1 . To the influence of changes of the dielectric constant of the medium with changing temperature and pressure, the

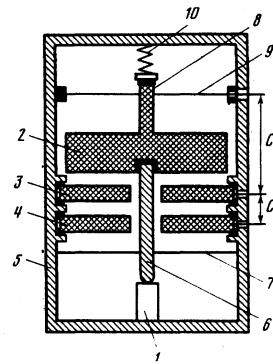


FIG. 1. Diagram of dilatometer with capacitive sensor.

change of the sample length was determined from the ratio of the variable capacitor C_1 to a reference capacitor C_0 made up of two immobile electrodes 3 and 4 (electrode 3 is common to the two capacitors). The entire set of electrodes, which are disk-shaped, is mounted inside the cylindrical shell 5 of the dilatometer. They are insulated from the shell by lines of thin (~ 0.05 mm) mica. Since the capacitances are measured by a three-electrode method, which eliminates in practice the influence of the capacitances to the shell, the insulation does not affect the measurement results. The moving electrode, a disk with two coaxial rods 6 and 8, is suspended on two specially shaped centering washers 7 and 9 that permit a 1-mm translational motion of the electrode without friction. The washers have low rigidity to axial displacements and are made of beryllium bronze sheet 0.07 mm thick. The push rod 6, which bears against the sample, is insulated from the disk and is connected to the shell through a centering washer 7. The lead from the moving electrode is the rod 8 together with washer 9, and bears through an insulator against the spring 10 that determines the pressure of the moving system on the sample. All the metallic parts of the dilatometer, including the shell, are made of a single stainless-steel stock part. The leads from the dilatometer electrodes are carefully screened. The capacitances are measured by a three-electrode scheme with a transformer bridge.¹⁵ The Tesla VM 400 (Czechoslovakia) bridge used by us has a resolution $\sim 2 \times 10^{-4}$ pF when an additional phase detector is used. The capacitances between the dilatometer electrodes amount to several picofarad. A change of 10 pF in the capacitor C_1 corresponds to a 100 Å change in the sample length. The slope of the dilatometer characteristic was determined accurate to 10% with a dial-type indicator. The initial sample length was measured prior to installation in the dilatometer, using a micrometer with accuracy ± 0.02 mm.

The dilatometer with the sample were placed in a beryllium-bronze high-pressure vessel with inside diameter 16 mm, designed for pressure up to 5 kbar. The pressure-transmitting medium was helium gas. The vessel was connected through a stainless-steel capillary to the high-pressure unit (Fig. 2). This unit comprised a compressor, a booster, a cylinder with manganin manometers, as well as a deflation valve with hydraulic drive for smooth pressure reduction. This installation is described in detail in Ref. 16; for our measurements it was supplemented with a pressure-stabilization system whose actuating element was a high-pressure vessel in which a heater was inserted. The heater was fed from a VRT-3 power regulator controlled through an F-118 preamplifier by the unbalance signal of a bridge with the manganin manometer in one of its arms. The pressure in the unit was measured with another manganin manometer calibrated against a UVD 15000 weight-and-piston manometer; the absolute calibration accuracy was ± 10 bar and the resolution of the pressure measuring instruments was 0.5 bar, and the pressure stability with the stabilizing system on did not exceed the resolution limits.

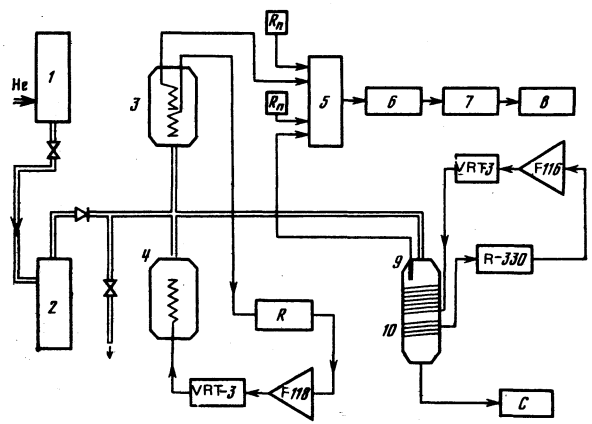


FIG. 2. Diagram of setup for dilatometric measurements at high pressures: 1—compressor, 2—booster, 3—high-pressure vessel with manganin manometers, 4—high-pressure vessel with heater of pressure stabilization system, 5—channel switching unit, 6—digital voltmeter, 7—electronic keyboard computer 15 VSM-5, 8—printing unit, 9—platinum thermometer, 10—high-pressure vessel with sample, R—resistance bridge, C—capacitance bridge, R_n —standard resistor.

The high-pressure vessel was placed in an evacuated volume which was placed in turn in a GK-200 cryostat. We wound around the high-pressure vessel a heater and the copper thermometer of the temperature-stabilization system, which consisted of an R-330 potentiometer, an F 116 amplifier, and a VRT-3 power regulator. With the volume evacuated, the high-pressure vessel temperature could be stabilized accurate to $\sim 10^{-3}$ K at any level, from liquid-nitrogen temperature to room temperature. The temperature of the high-pressure vessel was measured with a TSPN-1 platinum resistance thermometer mounted in vacuum grease in an opening in the vessel wall. To decrease the temperature gradients, the high-pressure vessel was surrounded with a copper screen; the temperature difference between the screen and the vessel was maintained constant. The time to reach thermal equilibrium in the high-pressure vessel was ~ 1 min. The resolution of the temperature-measurement system was better than 10^3 K, and the absolute calibration accuracy of the platinum thermometer was 0.01 K.

The resistances of the manganin manometer and of the platinum thermometer were measured by a four-contact method. The voltage drops on the manometer, thermometer, and standard resistors were recorded with a Solatron 7075 digital voltmeter (accurate to seven significant figures, resolution $0.1 \mu\text{V}$, input resistance higher than 100 GΩ), which was connected in succession to the signal sources through a measurement-channel switching system manufactured by the same firm. The data were transmitted directly to a 15 VSM-5 electronic keyboard computer to calculate the temperature and the pressure. The values of the pressure, temperature, and sample length were fed to a printout unit and were also recorded on magnetic tape for subsequent reduction.

EXPERIMENTAL RESULTS

The described technique was used to measure the lengths of SbSI samples along the c axis in the phase-transition region, in both the isothermal and the isobaric regime.

It turned out that the samples in our possession differed greatly in quality. Sample No. 1, grown from the gas phase, yielded poorly reproducible results even in regions far from the phase transition. The temperature interval of the first-order phase transition at atmospheric pressure reached 2 K for this sample. Sample No. 2, also obtained from the gas phase, had a much less smeared phase transition at atmospheric pressure, but at higher pressure its length still depended on the prior history of the sample. Sample No. 3, grown from the melt, was satisfactory in all respects (reproducibility of the length within the resolution limits of the instruments, the smearing of the transition at atmospheric pressure not higher than 0.02 K). Therefore all the data that follow pertain to this sample, with the exception of the SbSI phase diagram (Fig. 3), which was constructed using the transition temperatures and pressures of all three samples.

Figure 4 shows a family of isobars for sample No. 3; it is seen that above 240 K the transition is a well pronounced first-order transition with a distinct discontinuity of the length and with hysteresis. With decreasing temperature and increasing pressure of the transition, the length discontinuity and the hysteresis decreases, and below 220 K the ferroelectric-paraelectric phase transition in SbSI acquires all the features of a second-order phase transition without hysteresis or a length discontinuity. Figure 5 shows the dependence of the discontinuities of the length and of the temperature hysteresis on the transition temperature for sample No. 3. It is seen from the figure that both quantities tend to zero at ~ 233 K. Unfortunately, the

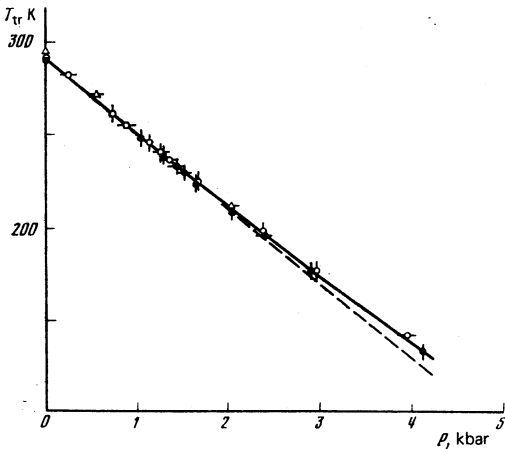


FIG. 3. Phase diagram of SbSI: Δ —sample No. 1, \circ —No. 2, \bullet —No. 3, horizontal bar—iso-therm, vertical bar—iso-bar. The transition points in the region of the second-order phase transitions were determined from the maximum of the derivative, and in the first-order transition region they were determined as the averages of the upper and lower hysteresis branches.

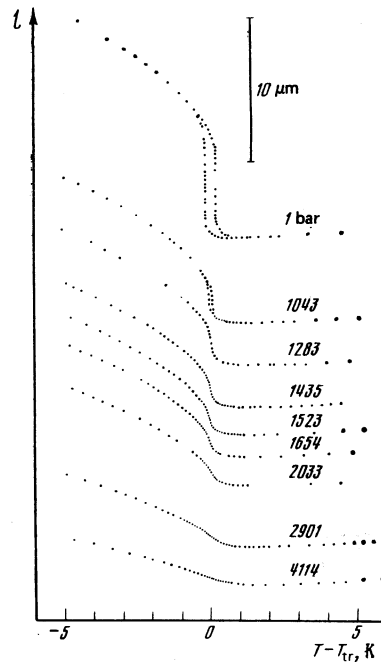


FIG. 4. Temperature dependence of the length of sample No. 3 at constant pressure at different pressures.

errors in the determinations of the discontinuities of the length and of the hysteresis do not make it possible to determine the temperature coordinate of the polycritical point with accuracy better than 5 K. Thus, according to our measurements, the coordinates of the polycritical point on the plot of the phase transition in SbSI are $T = 233 \pm 5$ K and $P = 1.42 \pm 0.1$ kbar. These data agree well with the results of Refs. 4 and 5.

The linear coefficient of thermal expansion and the linear compressibility were determined by numerically differentiating the initial experimental data. Figure 6 shows the temperature dependences of the coefficient of thermal expansion near the transition point for three values of the pressure—in the region of the first-order phase transition, near the polycritical point, and in the region where the phase transition is certainly of second order. Figure 7 shows plots of the linear compressibility against pressure near the phase transition in the critical region and in the region of the second-order transition. Figure 8 shows in log-log scale the

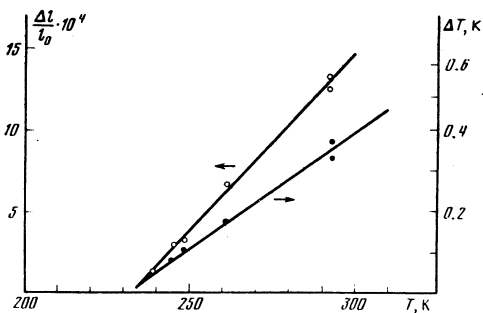


FIG. 5. Temperature dependences of the discontinuities Δl and of the L of the length and of the temperature hysteresis, respectively, for the phase transition in SbSI.

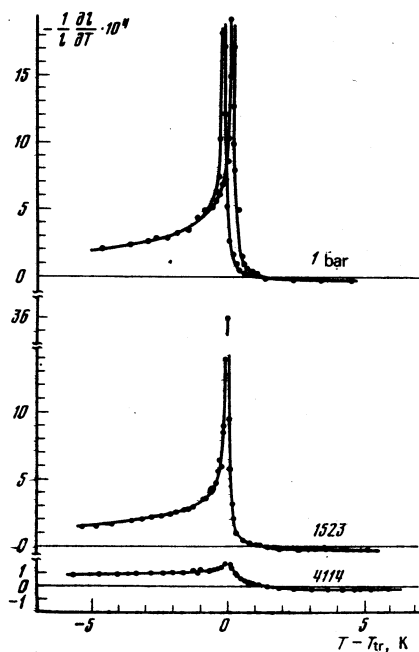


FIG. 6. Temperature dependence of the coefficient of linear expansion $l^{-1}dl/dT$ near the transition point, for three values of the pressure.

anomalous parts of the derivative of the length with respect to temperature

$$\left(\frac{\partial l}{\partial P}\right)_T^{\text{an}} = \left(\frac{\partial l}{\partial P}\right)_T - \left(\frac{\partial l}{\partial P}\right)_T^{\text{reg}}$$

in the ferroelectric phase as functions of $(T_{tr}-T)/T_{tr}$ for a number of isobaric sections. Measurements in far paraphase show that the regular part $(dl/dT)_P^{\text{reg}}$ can be regarded as constant.

Figure 9 shows an analogous plot for the derivative of the length with respect to pressure

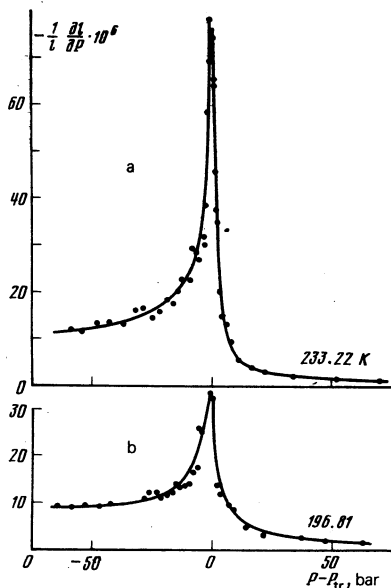


FIG. 7. Dependence of the linear compressibility $l^{-1}dl/dP$ on the pressure for two values of the temperature: a—in the polycritical region, b—in the region of the second-order transition.

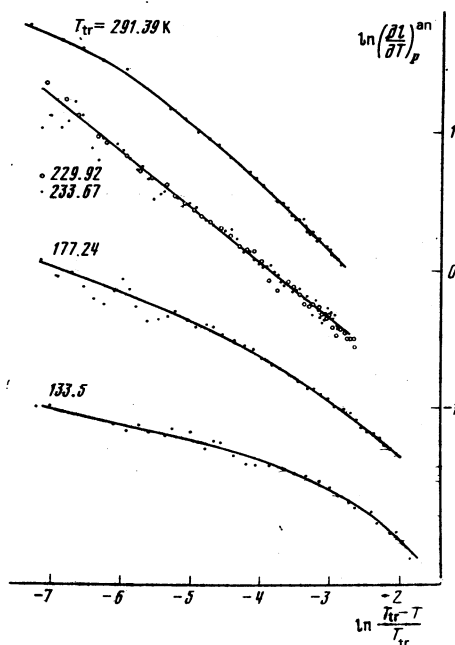


FIG. 8. Temperature dependence of the anomalous part of the derivative $(\partial l/\partial T)_P$ in the vicinity of the phase transition point in the ferroelectric phase (logarithmic scale).

$$\left(\frac{\partial l}{\partial T}\right)_P^{\text{an}} = \left(\frac{\partial l}{\partial T}\right)_P - \left(\frac{\partial l}{\partial T}\right)_P^{\text{reg}}$$

in the ferroelectric phase as a function of $(P_{tr}-P)/P_{tr}$ for two temperatures close to critical. In this case the regular part was chosen in the form $c + c'P$. As seen from the plots in Figs. 8 and 9, the behavior of the anomalous parts of both derivatives in the critical region can be well described in the form

$$\left(\frac{\partial y}{\partial x}\right)^{\text{an}} \sim \left(\frac{x_{tr}-x}{x_{tr}}\right)^{-\alpha}$$

with exponents $\alpha_T = 0.41$ and $\alpha_P = 0.83$ corresponding respectively to the isobaric and isothermal sections. The confidence intervals of α_T and α_P with account taken of the errors in the determination of the regular parts of the thermal expansion and of the compressibility are $\delta\alpha_T \approx 0.03$ and $\delta\alpha_P \approx 0.05$ at a 95% probability level, so that the differences between the estimates of α_T and α_P can be disregarded.

DISCUSSION OF RESULTS

The obtained values of the exponent α show that the polycritical point on the phase-transition curve is of order not higher than third, since $\alpha = 0.67$ already for

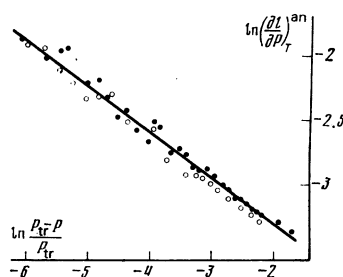


FIG. 9. Dependence of the anomalous part of the derivative $(\partial l/\partial P)_T$ on the pressure in the vicinity of the critical point at $T = 230.01$ K (points \circ) and 233.32 K (points \bullet) in logarithmic scale.

the tetracritical point (the value of the exponent increases monotonically with increasing order of the polycritical point). We note, however, that this exponent is still lower than the $\alpha = 0.5$ which follows from the Landau theory. This difference can be due to a number of causes, such as 1: (1) the presence of impurities and defects in the sample, (2) incorrect choice of the regular parts of the corresponding quantities, and (3) disparity between the trajectory on which the tricritical point is approached and the Landau theory. The last cause seems to us to be the most significant.²⁾ In fact, a relation such as (2) for the anomalous parts of the corresponding derivatives, with an exponent $\alpha = 0.5$, was obtained by putting $B = 0$ in Eq. (1). This means that the trajectory that approaches the tricritical point should have a direction corresponding to $B = 0$, but unfortunately this can not be realized beforehand. Consequently, in the analysis of the results of the isothermal and isobaric measurements must be taken into account that the coefficient B in (1) is not identically equal to zero.

We now write down the first terms of the expansions of the coefficients A and B from (1) near the tricritical point in the form

$$\begin{aligned} A &= a_1(T - T_t) + a_2(P - P_t) + \dots, \\ B &= b_1(T - T_t) + b_2(P - P_t) + \dots \end{aligned} \quad (3)$$

Substituting (3) in (1) we readily obtain for the derivative V/T the expression

$$\begin{aligned} \left(\frac{\partial V}{\partial T}\right)_P &= \left(\frac{\partial V}{\partial T}\right)_P^{\text{reg}} + \beta_0 + \beta_1 |T - T_t|^{-0.5} + \beta_2 |T - T_t|^{0.5}; \\ \beta_0 &= -\frac{a_2 b_1 + a_1 b_2}{3D}, \quad \beta_1 = -\frac{a_1 a_2}{2(3a_1 D_2)^{1/2}}, \\ \beta_2 &= -\frac{3}{4} \frac{a_2 b_2}{a_1^{1/2} (3D)^{3/4}} - 3 \frac{b_1 b_2 a_1^{1/2}}{(3D)^{3/4}}. \end{aligned} \quad (4)$$

A similar expression is obtained for the derivative $(\partial V / \partial P)_T$. Thus, the linear compressibility and the coefficient of thermal expansion take near the tricritical point the form

$$\kappa = \kappa_0 + \kappa_1 \left| \frac{x - x_t}{x_t} \right|^{-0.5} + \kappa_2 \left| \frac{x - x_t}{x_t} \right|^{0.5} \quad (5)$$

The square-root term in (5) is not small and must be taken into consideration in the reduction of the experimental data. A search for the exponent α in the sense of the best mean-squared approximation at fixed values of T_T for two tricritical isobars in an expression of the form (5) yielded the values $\alpha_T = 0.50$ and 0.53 . The corresponding search for the exponent α in the expression for the linear compressibility along one tricritical isotherm yielded $\alpha_P = 0.55$. The confidence intervals for the indicated values of α_T and α_P lie in the range $\delta\alpha \approx 0.03 - 0.05$ for the 95% level, so that the scatter of the values of α conforms with the experimental accuracy.

Using an expression in the form (5) for the linear expansion and the compressibility, a search was made also for the best values of T_t and P_t . The resultant T_t and P_t differ from the experimental ones by values on the order of 0.01 K and 1 bar, a result comparable with the smearing of the corresponding peaks at the phase-transition point.

Summarizing, we can state that within the limits of experimental accuracy the exponent α determined by us does not differ with the $\alpha = 0.5$ predicted by the Landau theory for the tricritical point. It must be noted that in the presence of anomalies on the side of the paraelectric phase (see Figs. 6 and 7) does not mean that the Landau theory cannot be used in this region. The most that the presence of hysteresis in this region can indicate, when the phase transition is still of first order, is that there exist individual sections of the ferroelectric phase, imbedded in the paraphase and resulting from defects of various kinds.

¹High-Temperature Institute, USSR Academy of Sciences.

²The fluctuation corrections should also influence the value of the exponent, but for the reasons stated in the introduction their effect should be small in our case. At any rate the fluctuation corrections should increase the effective value of the exponent.

¹L. D. Landau, Phys. Zs. Sovjet. **8**, 113 (1935). L. D. Landau, Sobranie trudov (Collected Works), Vol. 1, Nauka, 1969, p. 123 [Pergamon].

²L. Benguigi, Phys. Stat. Sol. (b) **60**, 835 (1973).

³T. R. Volk, E. I. Gerzanich, and V. M. Fridkin, Izv. AN SSSR, ser. fiz. **33**, 348 (1969).

⁴C. W. Garland and B. B. Weiner, Phys. Rev. B **3**, 1634 (1971).

⁵R. B. Griffiths, Phys. Rev. Lett. **24**, 715 (1970).

⁶C. W. Garland and J. D. Baloga, Phys. Rev. B **16**, 331 (1977).

⁷V. H. Schmidt, A. B. Western, and A. G. Baker, Phys. Rev. Lett. **37**, 839 (1976).

⁸R. Clarke and L. Benguigi, Solid State Phys. **10**, 1963 (1977).

⁹L. D. Landau and E. M. Lifshitz, Statisticheskaya fizika (Statistical Physics), Nauka, 1976 [Pergamon].

¹⁰A. P. Levanyuk and A. A. Sobyenin, Pis'ma Zh. Eksp. Teor. Fiz. **11**, 540 (1970) [JETP Lett. **11**, 37 (1970)].

¹¹L. N. Syrkin, I. N. Polandov, N. P. Kachalov, and E. V. Gamynin, Fiz. Tverd. Tela (Leningrad **14**, 610 (1972) [Sov. Phys. Solid State **14**, 517 (1972)]).

¹²G. A. Samara, Ferroelectrics **9**, 209 (1975).

¹³P. S. Peercy, Phys. Rev. Lett. **35**, 1581 (1975).

¹⁴G. A. Samara, Phys. Rev. B **17**, 3029 (1978).

¹⁵A. M. Thomson, IRE Trans., Instr. I-7, 245 (1958).

¹⁶S. M. Stishov and A. F. Uvarov, Prib. Tekh. Éksp. No. 4 191 (1975).

Translated by J. G. Adashko